Charge Density Study using Low Electrode Diameter in Epiretinal Prosthesis

Diego Luján Villarreal, Dietmar Schroeder and Wolfgang H. Krautschneider.

***Abstract*—Reducing electrode size can be advantageous for stimulating the retina because they produce focal stimulation, i.e. one active electrode excites a single cell thereby greatly increasing resolution. The main limitation is, however, the high charge density of low electrode area that can cause adverse tissue reactions. In this study, we analyze the use of rectangular and linear increase pulse shapes based on charge injection capacity, voltage window and threshold current using a single ganglion cell model with PEDOT-NaPSS arranged electrode array. We found that 100µs linear increase pulse shape delivers a better response of charge density and electrode potential than rectangular that would avoid irreversible Faradaic reactions.**

***Index Terms*—charge injection capacity, linear increase pulse, low electrode, rectangular pulse shape, retinal implant, voltage window.**

I. INTRODUCTION

RETINAL prosthetic devices have strived to replace the functionality of photoreceptors lost because of degenerative diseases such as retinitis pigmentosa (RP) or age-related macular degeneration (AMD). These diseases are incurable by current treatments. Although the ability to create visual sensations is now well established [1], the quality of vision elicited by retinal implants is facing further challenges for safely electrode implantation.

Decreasing electrode dimensions will allow focal excitation of small groups of cells that lead to high resolution patterns of prosthetic-elicited activity and improve visual reception. This challenge, however, requires higher charge density that can cause breakdown of the electrode as well as adverse tissue reactions [2].

The electrochemical reactions at the electrode-tissue interface, i.e. capacitive double-layer charging, reversible Faradaic and irreversible Faradaic reactions, carry out charge injection into the neural tissue [3,4,5]. The latter reaction can produce electrolysis of water that leads to localized pH changes [6], gas bubble formation that thought to be harmful and physically disturbs the tissue [4, 5] and chemical species formation that damage the tissue or the electrode [3].

Manuscript received month, day, 2016; revised month, day, 2016; accepted month, day, 2016.

Diego Lujan Villarreal, Dietmar Schroeder and Wolfgang H. Krautschneider are with the institute of Nano and Medical Electronics at the Hamburg University of Technology (corresponding author phone: +49 40 42878 3991; fax +49 40 42878 2877

Having as a rule of thumb that one should avoid the onset of irreversible Faradaic processes when designing electrical stimulation systems, this would impose to keep the injected charge density at a low level within reversible charge injection processes.

A novel strategy has been proposed [3] that generally suggest keeping the pulse width narrower because it confines the amount of current that can be delivered by a stimulator, especially if it is battery operated, and provides the minimum charge that occurs when pulse width is of tens of µs.

There is evidence that single linear increase pulse shape at lower pulse durations can deliver lower charge than rectangular, linear decrease and sinusoidal pulse shapes [7].

Furthermore, electrolysis of water occurs as a result when maximum cathodic and anodic potential across the electrodes surpass the "water window" boundary [8]. The water window is a potential range that is defined by the reduction of water, forming hydrogen gas, in the negative direction, and the oxidation of water, forming oxygen, in the positive direction which may cause corrosion.

Once the electrode potential attains either of these two voltage window boundaries, all further injected charge goes into the irreversible Faradaic processes of water oxidation or water reduction [3].

PEDOT is a conductive polymer has been generated considerable attention as a supercapacitor material due to its large electroactive voltage window, high chemical stability among conductive polymers [9], lower impedance and higher charge injection capacity, Q_{INJ} [10]. Q_{INJ} is defined as the amount of charge per unit area that can be delivered through an electrode without causing water electrolysis.

The aim of this study is to investigate the use of rectangular and linear increase pulse shapes based on charge injection capacity, voltage window and threshold current using a single ganglion cell model with PEDOT-NaPSS arranged electrode array. We give some advice on carrying out efficient stimulation by avoiding damage to the tissue and to the electrode.

II. METHODS

A. Ganglion Cell Model

Ganglion cell model has a basic mathematical structure for voltage-gating based on Hodgkin and Huxley like equations [11] and is modelled with an equivalent circuit taken from previously published model of repetitive firing of retinal ganglion cells [12]. The parameters and equations that describe the dynamics of the ionic channels were kept as in the original model.

B. Retinal Model

We used the identical COMSOL model of the retina as seen in [13]. The model is shown in figure 1.

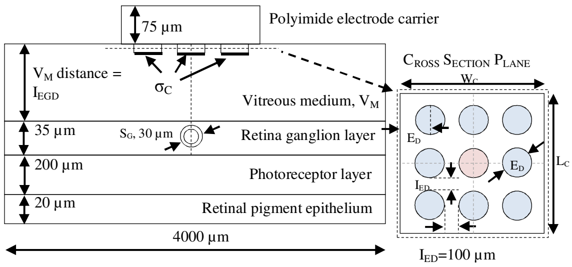

Fig. 1. Retina model at COMSOL simulations. Layer thicknesses not drawn to scale

It consists of seven domains: polyimide carrier of electrodes P_C; vitreous medium V_M; retina ganglion cell layer R_{GC}; photoreceptor layer P_{RC}; retinal pigment epithelium R_{PE}; ganglion cell soma S_G and the electrode array E_{ELE}. The ganglion cell soma was placed inside the retina ganglion cell layer exactly below the center of active electrode and was enclosed with the cell membrane.

The material coating the electrode is PEDOT-NaPSS electrodeposited in gold electrodes with a charge density of 40 mC/cm^2 as seen in [10].

The electrode array configuration is shown at the cross section plane in figure 1. This arrangement is analogous to [14,15] however it consists of an active electrode (in red) surrounded by eight guards (in blue) in order to stress the isolation of the active electrode, to confine the stimulus current to a small volume around the ganglion cell and to minimize electrode cross-talk during stimulation.

C. Simulation Procedure – Ganglion Cell Model (Matlab)

In this work we used the identical ganglion cell model as in [12] to calculate in Matlab the extracellular threshold current density of the ganglion cell by applying monophasic rectangular and linear increase pulse shapes to the model at 500 pulses per second, taking into account absolute and refractory period of an action potential.

We followed the strategy as seen in [3] and we chose two pulse duration, Δt, of 50 and 100 µs. Pulse widths lower than 150 µs are analogous in [2] to directly stimulate the ganglion cell and to elicit solely a single spike with precise temporal pattern. The peak current density amplitude was swept with a resolution of 1 µA/cm^2 until it was found the threshold current density that fires a train of action potential.

The result of extracellular peak current amplitude are 330 and 120 µA/cm^2 for rectangular pulse shape and 340 and 160 µA/cm^2 for linear increase at 50 and 100 µs, respectively.

D. Simulation Procedure – Retinal 3D Model (COMSOL)

The retinal modelling was built in COMSOL and shown in figure 1. In this work we used the identical retinal model as in [13].

The ganglion cell soma was placed inside the retina ganglion cell layer exactly below the center of active electrode and was enclosed with the cell membrane.

In previous published works [16,17,18,19,20] there have been sufficient evidence that monophasic pulse allows the formation of Faradaic reduction reactions. If oxygen is presence, these reactions may include reduction of oxygen and formation of reactive oxygen species associated in tissue damage.

Although monophasic is the most efficient pulse for stimulation because of the action potential initiation and the potential becomes insufficiently positive (using cathodic pulses) where electrode corrosion may occur, however, it is not used in continuous pulses where tissue damage is to be avoided [3].

We used, however, monophasic rectangular and linear increase shapes with a single anodic pulse for the solely intention to reduce the computational time consumed.

We iterated the retinal model for each E_D, I_{EGD} and Δt until we match the average boundary current density of the cell with the extracellular threshold current amplitude obtained in Matlab by applying current from the active electrode.

We assumed that the irreversible Faradaic reactions, if present, will occur such that the charge density surpass the Q_{INJ} limit or the anodic peak potential at the electrode surpass the voltage window boundary.

The inter electrode ganglion cell distance, $I_{EGD,}$ are 2, 10, 100 µm. The electrode diameter, E_D, are 2, 10 50, 100 µm. The Δt are 50 and 100 µs. We briefly analyzed pulse duration of 150 µs and yielded the highest charge density than 50 and 100 µs.

Out of COMSOL simulations, we also obtained the voltage across the electrodes over time.

E. Charge Density CalculationI

The charge density was obtained by integrating the current delivered by the active electrode over time and dividing it by the electrode area. It is worth to mention that all eight surrounding electrodes including the active changed their dimensions accordingly.

Q_{INJ} of gold microelectrode coated with PEDOT-NaPSS follows a linear relationship with charge density used during electropolymerization, Q_D, with a constant 0.075 Q_{INJ} per Q_D (until 300mC/cm^2) for 0.001 and 1 mm^2 electrode size [10].

Q_{INJ} may also be increased by increasing electrochemical surface area [21].

As there is no evidence about Q_{INJ} in PEDOT-NaPSS low electrode area, we used the limit of 0.35 mC/cm^2 for gas-free and erosion-free operation [4] and 1mC/cm^2 for neural damage [22].

F. Voltage Window Boundary

PEDOT voltage window extends beyond conductive materials, such as MnO_2, from 1.5 V [23] up to 1.7 V [9].

As there is no evidence about voltage window on PEDOT-

NaPSS low electrode area, we used the limit of 1.7 V.

III. Results

A. *Charge Density Results*

Figures 2 to 4 show the comparison of threshold charge density, left y-axis, and the threshold current for ganglion cell activation, right y-axis, for monophasic rectangular and linear increase pulse shapes.

Each plot shows the results for a specific I_{EGD}. On top of each plot the forbidden region of gas formation and neural damage are shown with a red dashed-line.

Table I lists the minimum electrode diameter [µm] that can be used with their corresponding limit.

The green boxes indicate the suitability to use the minimum electrode diameter tested of 2 µm.

TABLE I
Charge Density Limits for Rectangular/Linear Increase Pulse Shapes

I_{EGD}	0.35 mC/cm^2 limit		1 mC/cm^2 limit	
	50 µs	100 µs	50 µs	100 µs
2 µm	Yes/Yes	Yes/Yes	Yes/Yes	Yes/Yes
10 µm	Yes/Yes	Yes/Yes	Yes/Yes	Yes/Yes
100 µm	18/9.9	14/9.9	9.7/9.3	9.6/9.3

For a successful implant of retinal device, only the lower safe charge density of 0.35mC/cm^2 should be employed.

B. *Voltage across Electrodes Results*

Figures 5 and 6 illustrate the comparison of voltage across the electrodes. Each plot shows the results for a specific I_{EGD}.

On top of each plot the voltage window boundary is shown with a red dashed-line.

Table II lists the minimum electrode diameter [µm] that can be used for the corresponding limit.

TABLE II
Voltage Limits for Pulse Shapes

I_{EGD}	Rectangular		Linear Increase	
	50 µs	100 µs	50 µs	100 µs
2 µm	Yes	Yes	Yes	Yes
10 µm	Yes	Yes	Yes	Yes
100 µm	9	4.42	9.2	6.3

The green boxes indicate the suitability to use the minimum electrode diameter tested of 2 µm.

IV. Discussion

A. *Threshold Current*

Threshold currents, figures 2 to 4, were found to increase with time after surgery, most likely due to the lifting off of the electrode array from the retinal surface [24].

Threshold variations with respect to I_{EGD} are consistent with previous experimental work of epiretinal device implanted in rabbits [25].

Because linear increase shape injects less charge than rectangular for a given pulse duration, the former necessitates a higher amplitude to reach threshold.

B. *Charge Density*

It is evident that the charge density, figures 2 to 4, decreases using linear increase pulse shape.

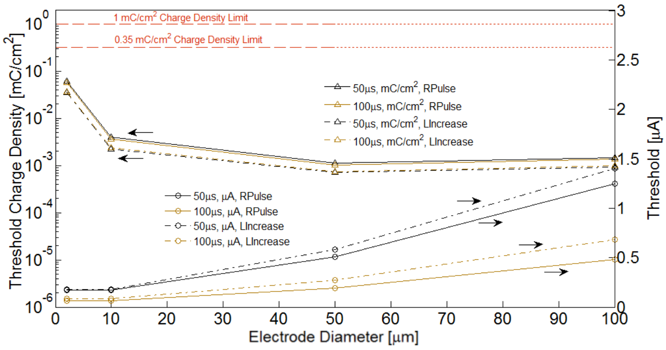

Fig. 2. Threshold charge density and threshold current for 2 µm inter electrode-ganglion cell distance.

Using 50 µs pulse duration, charge density is reduced up to 40±2.4% in average; for 100 µs, it is decreased 30±1.3%. This means a promising technique to avoid irreversible Faradaic reactions.

The rectangular pulse shape has its own attributes meaning that using E_D of 2 µm, 50 or 100 µs pulse duration, and I_{EGD} lower than 10 µm is safe within the limits. This technique works with linear increase pulse shape as well. Doing so, it provides a method to send a more natural signal to the brain and to generate meaningful percepts.

Figure 4 show the constraint of charge density at both limits mainly when I_{EGD} is greater than 10 µm.

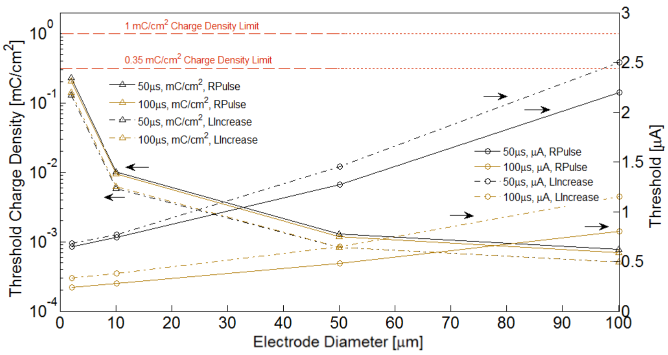

Fig. 3. Threshold charge density and threshold current for 10 µm inter electrode-ganglion cell distance.

For achieving a better response in continuous pulses, charge-imbalanced biphasic waveform provides a method to reduce the irreversible charge density as reactions occurring in one phase (cathodic or anodic) are reverse in the following [3].

Furthermore, it was demonstrated that this waveform allows greater cathodic charge densities than monophasic prior to the onset of tissue damage [26].

C. *Voltage across Electrodes*

It is also evident that using 100 µs pulse duration, more than one third but less than half of electrode voltage, fig. 5 and 6, is reduced than 50 µs for both pulse shapes. This technique would avoid irreversible Faradaic reactions.

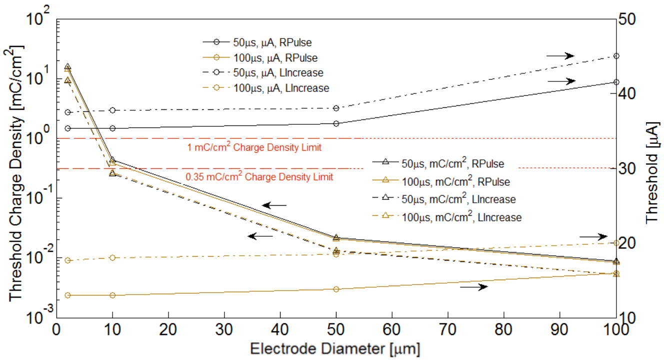

Fig. 4. Threshold charge density and threshold current for 100 µm inter electrode-ganglion cell distance.

Considering figure 5 and 6, we learn that it is safe to work with E_D of 2 µm, low pulse durations lower than 150 µs, I_{EGD} lower than 10 µm with either rectangular or linear increase pulse shapes.

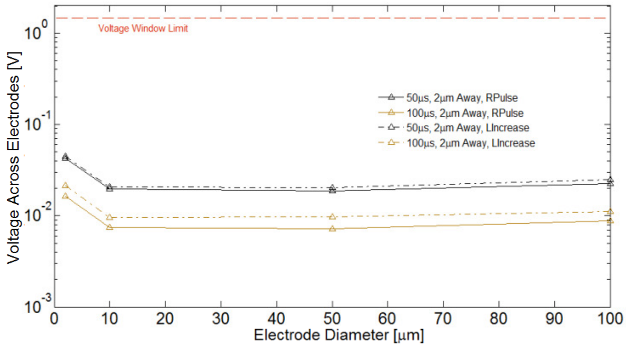

Fig. 5. Voltage results for 2 µm inter electrode-ganglion cell distance for rectangular and linear increase pulse shapes.

Figure 6 show that the constraint of voltage window limit originates mainly when I_{EGD} is greater than 10 µm.

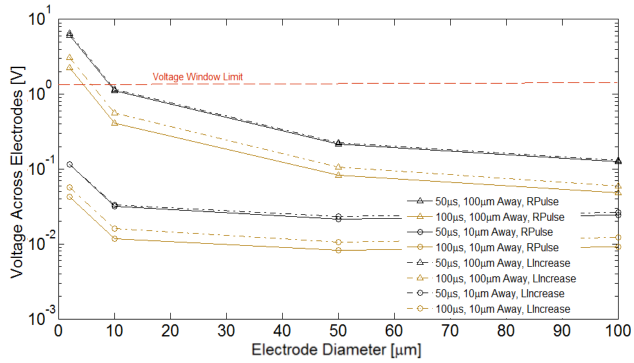

Fig. 6. Voltage results for 10 and 100 µm inter electrode-ganglion cell distance for rectangular and linear increase pulse shapes.

It should be noted that in fact irreversible processes might occur at potentials within the voltage window, such as irreversible oxygen reduction, as opposed to the opinion in many studies that states reversible charge storage capacity, or Q_{INJ}, can be applied without the electrode potential exceeds the voltage window during pulsing [3]. Therefore, Q_{INJ} and voltage window limits need to be analyzed separately.

For attaining a better response in successive pulses, the charge-imbalanced waveform has advantages in avoiding corrosion by decreasing the maximum positive potential since the anodic phase is no longer constrained to be equal to the cathodic phase as charge-balanced pulse, thus the electrode potential reaches less positive values [3,26].

V. Conclusions

We found that 100µs linear increase pulse shape delivers a better response of charge density and electrode potential than rectangular that would avoid irreversible Faradaic reactions.

Furthermore, for a given I_{EGD} with charge density limit of $0.35 mC/cm^2$ and voltage window limit of 1.7V, our model suggests:

i) $0<I_{EGD}<10$ µm: a) reduce electrode diameter to 2 µm; b) work with either 50 or 100 µs low pulse duration; c) use either rectangular or linear increase pulse shapes.

ii) $10<I_{EGD}<100$ µm (for rectangular pulse): a) reduce electrode diameter to 14 µm only with 100 µs pulse duration. For 50 µs, electrode diameter should be 18 µm.

iii) $10<I_{EGD}<100$ µm (for linear increase pulse): a) reduce electrode diameter to ~10 µm with either 50 or 100 µs pulse duration.

If pulse trains are needed, the charge-imbalanced waveform has added advantages in avoiding corrosion and reducing irreversible charge densities that leads to either electrode or tissue damage [3,26].

Additional experimental testing of small electrodes is still required to verify our results. Moreover, further simulations of heat dissipation should be performed to verify the use of 1000+ electrode array for epi- or subretinal implants.

References

[1] Cai, Qiushi, et al. Response variability to high rates of electric stimulation in retinal ganglion cells. J Neurophysiology, 2011.

[2] Fried S., et al. A Method for Generating Precise Temporal Patterns of Retinal Spiking Using Prosthetic Stimulation. J Neurophysiol 95: 970–978, 2006.

[3] D. R. Merrill, M. Bikson, and J. G. Jefferys, "Electrical stimulation of excitable tissue: Design of efficacious and safe protocols,"J. Neurosci. Methods , vol. 141, no. 2, pp. 171–198, Feb. 15, 2005.

[4] S. B. Brummer and M. J. Turner, "Electrochemical considerations for safe electrical stimulation of the nervous system with platinum electrodes," IEEE Trans. Biomed. Eng., vol. 24, no. 1, pp. 59–63, Jan. 1977.

[5] S. F. Cogan, "Neural stimulation and recording electrodes," Annu. Rev. Biomed. Eng., vol. 10, pp. 275–309, 2008.

[6] C. Q. Huang, P. M. Carter, and R. K. Shepherd, "Stimulus induced pH changes in cochlear implants: An in vitro and in vivo study," Ann. Biomed. Eng., vol. 29, no. 9, pp. 791–802, Sep. 2001.

[7] Mario A. Meza-Cuevas, Dietmar Schroeder and Wolfgang H. Krautschneider. Neuromuscular Electrical Stimulation Using Different Waveforms - Properties comparison by applying single pulses. 5th International Conference on BioMedical Engineering and Informatics, 2012.

[8] Ronald T. Leung, Mohit N. Shivdasani, David A. X. Nayagam, Robert K. Shepherd. In Vivo and In Vitro Comparison of the Charge Injection Capacity of Platinum Macroelectrodes. IEEE Transactions on Biomedical Engineering, Vol. 62, No. 3, March 2015.

[9] Jonathon Duay, Eleanor Gillette, Ran Liu, Sang Bok Lee. Highly flexible pseudocapacitor based on freestanding heterogeneous MnO2/conductive polymer nanowire arrays. Phys. Chem. Chem. Phys., 2012, 14, 3329–3337.

[10] Starbird, R. et al. Electrochemical properties of PEDOT-NaPSS galvanostatically deposited from an aqueous micellar media for invasive electrodes, IEEE BMEICON, 2012.
[11] Hodgkin A., et al. A quantitative description of membrane current and its application to conduction and excitation in nerve. J. Physiol, 1952.
[12] Fohlmeister J., et al. Modeling the repetitive firing of retinal ganglion cells. Brain Research, 1989.
[13] Lujan Villarreal D., et al. "Feasibility Study of a 1000+ Electrode Array in Epiretinal Prosthesis." (Forthcoming, 2016) 8th International Conference on Bioinformatics and Biomedical Technology. Barcelona, Spain. June 10-12, 2016.
[14] Lovell N., et al. Current distribution during parallel stimulation: Implications for an epiretinal neuroprosthesis. IEEE Eng Med Biol Soc, 2005.
[15] Dommel N., et al. A CMOS retinal neurostimulator capable of focussed, simultaneous stimulation J Neural Eng, vol. 6, pp. 035006, 2009.
[16] Halliwell B. Reactive oxygen species and the central nervous system. J Neurochem 1992;59(5):1609–23.
[17] Imlay JA. Pathways of oxidative damage. Annu Rev Microbiol 2003;57:395–418.
[18] Bergamini CM, Gambetti S, Dondi A, Cervellati C. Oxygen, reactive oxygen species and tissue damage. Curr Pharm Des 2004;10(14):1611–26.
[19] Stohs SJ. The role of free radicals in toxicity and disease. J Basic Clin Physiol Pharmacol 1995;6(3–4):205–28.
[20] Hemnani T, Parihar MS. Reactive oxygen species and oxidative DNA damage. Indian J Physiol Pharmacol 1998;42(4):440–52.
[21] Mario A. Meza-Cuevas. Stimulation of Neurons by Electrical Means. Logos Verlag Berlin GmbH. 2015.
[22] Warren E. Finn, et al. Handbook of Neuroprosthetic Methods. CRC Press, Dec 16, 2002.
[23] Boretius, T., M. Schuettler, and T. Stieglitz. On the Stability of PEDOT as Coating Material for Active Neural Implants. 15th Annual Conference of the International Functional Electrical Stimulation Society, 2010.
[24] Chader G., et al. Artificial vision: needs, functioning, and testing of retinal electronic prosthesis. Progress Brain Research, Vol. 175, 2009.
[25] Jensen R., et al. Thresholds for Activation of Rabbit Retinal Ganglion Cells with Relatively Large, Extracellular Microelectrodes. IOVS, 2005.
[26] Scheiner A, Mortimer JT. Imbalanced biphasic electrical stimulation: muscle tissue damage. Ann Biomed Eng 1990.

Diego Lujan Villarreal was born in Monterrey, Nuevo León, México in 1983. He received the B.S. degree in Mechatronics from the Monterrey Institute of Technology and Higher Education (ITESM) in 2006 and the M.S. degree in Microelectronics and Microsystems from the Hamburg University of Technology in 2010.

He has worked with the Cellular Therapy Department in the School of Medicine at ITESM, Monterrey, México, and he is now pursuing his PhD in the Institute of Nano and Medical Electronics at the Hamburg University of Technology, Hamburg, Germany.

His main research interests focus on theoretical models of neurostimulation, optimal energy-saving algorithms and epi- and sub retinal stimulation.

Dietmar Schroeder (M'88–SM'94) received the Dr. Ing. degree in electrical engineering from the Technische Universität Braunschweig, Braunschweig, Germany, in 1984.

He joined the Hamburg University of Technology, Hamburg, Germany, in 1983, where he has been a Lecturer with Semiconductor Electronics since 1994.

Wolfgang H. Krautschneider (M'85) received the M.Sc., Ph.D., and Habilitation degrees from the Berlin University of Technology, Berlin, Germany.

He was with Central Research Laboratories, IBM, Yorktown Heights, NY, USA, the Siemens Research Center, Munich, Germany, and the DRAM Project of IBM and Siemens, Essex Junction, VT, USA.

He is currently the Head of the Institute of Nano and Medical Electronics at the Hamburg University of Technology, Hamburg, Germany.